Pools of water in anhydrobiotic organisms

A thermally stimulated depolarization current study

Fabio Bruni*‡ and A. Carl Leopold§

* Section of Plant Biology and § Boyce-Thompson Institute, Cornell University, Ithaca, New York 14853 USA

ABSTRACT The ability to survive the removal of water in anhydrous biosystems is especially remarkable as a departure from the manifold structural and functional dependences on the presence of H_2O molecules. Identifiable pools of water present in dry soybean axes were investigated by means of the thermally stimulated depolarization current method. Samples were examined in the temperature range 100–340 K and over water contents (h, in gram H_2O per gram sample dry weight) ranging from h = 0.05 to 0.30 g/g. Three water-dependent relaxation mechanisms were detected; one attributed to dipolar reorientation of H_2O molecules hydrogen-bonded to other water molecules, one to reorientation of CH_2OH groups, and one to a glass transition in sugar-water domains. These glassy domains can protect intracellular components against destruction in the dehydrated state. Interestingly, protecting glassy domains were not found in dehydration intolerant seeds, supporting the hypothesis that the ability to withstand dehydration is associated with intracellular glass formation. A model for the state of cell water at interfaces is proposed.

INTRODUCTION

In the evolution of life systems, water has been a component of transcendent importance. Water is in fact one of the essential components of life, and its functions are manifold. At the microscopic level, discrete H_2O molecules or small aggregates are implicated in the maintenance of biologically active conformations of nucleotides, proteins, and carbohydrates. Macrostructures, such as membranes, are stabilized and sustained by the presence of critical numbers of bound water molecules (1). In metabolism and synthesis, H_2O is the universal reagent in any process that involves hydrolysis, condensation, reduction, or oxidation, and that includes most biochemical reactions.

The ability to survive the removal of water in anhydrous biosystems is especially remarkable as a departure from the above structural, as well as functional, dependences (2). Anhydrous biosystems include plant seeds, spores, pollen grains, bacteria, cysts of desiccated forms of organisms, such as the brine shrimp *Artemia,* and certain nematodes.

It is not uncommon that organisms with unusual features provide unique advantages for the study of specific problems. The physical properties of water in anhydrous multicellular organisms represent one of these problems, and for the extent with which its experimentally determined properties differ from its behavior when in bulk aqueous solutions, water is without peer (3).

Previous studies on dry biological systems indicated that the physical properties of water molecules change discretely with hydration level (4–7). From such data, models analogous to those proposed for the hydration of single macromolecules (8) have been developed to describe hydration of tissues. In general terms, the existence of three types of interfacial water has been postulated: strongly bound water at low water contents, weakly bound water at intermediate water contents, and very loosely bound water at higher water contents. Figures for the above regions of water content (h, in gram water per gram dry sample) vary with experimental sample, generally being below h = 0.1 g/g for the strongly bound water, between h = 0.1 and 0.2 for the intermediate, and greater than h = 0.2 for the very loosely bound water. Recent dielectric studies underlined the role of water protons moving along chains of hydrogen-bonded H_2O molecules in triggering metabolic events (9–11). This information has given further support to the idea that the above regions of water content are strictly connected to the onset of sample-specific biological functions.

The possibility that some of these water pools may be associated with aqueous glasses in the cytoplasm of anhydrous systems, even at physiological temperatures, lately has been put forward (12) and has, since then, gained supporting experimental evidence (13–16). The existence of such glassy phase is particularly relevant to anhydrous biology. A glass is a liquid of high viscosity, such that it stops or slows down all chemical reactions requiring molecular diffusion (17). In so doing, a glassy state may assure quiescence and stability over time. Moreover, a glassy state could represent a useful mechanism to trap residual water molecules and to prevent damaging interactions between cell components (12). In addition, the resulting highly viscous phase can be readily liquefied on addition of water, thus restoring the possibility for metabolic activities.

The purpose of this paper is to further analyze the physical properties of pools of water molecules at biological interfaces using thermally stimulated depolarization current (TSDC) measurements in the temperature range

‡ Address correspondence to Fabio Bruni, Dipartimento di Fisica, Università di Roma "La Sapienza", 00185 Rome, Italy.

0006-3495/92/09/663/10 $2.00

of 100–340 K and over water contents ranging from h = 0.05 to 0.30 g/g. Properties of water molecules in this hydration range are critical for anhydrobiotic organisms, and it is within this range that desiccation tolerant systems are switched from physiologically inactive to physiologically active states (5, 11, 18). In view of this objective, the TSDC technique is especially suited because of its ability to experimentally analyze complex relaxation processes arising from a distribution of relaxation times (19, 20). Moreover, a TSDC spectrum recorded in the above temperature range can comprise several distinct relaxation events measured on the same sample and with the same contact configuration, which in AC methods would correspond to a frequency range from several gigahertz to a few millihertz, a range impossible to cover with any other single experimental arrangement.

MATERIALS AND METHODS

Soybean seed (*Glycine* max L.) was selected because there are existing data on its hydration properties (4, 7), as well as on its hydration-dependent glass transition (15). Axes of soybean seed were hand dissected. Samples weighing ~200 mg were dehydrated over P_2O_5 under vacuum for 12 h, after which sample water content was adjusted by incubating over saturated salt solutions at 5°C until constant weight was achieved (5 d) (11). The amount of water taken up by the sample at equilibrium was determined gravimetrically, and the sample was then used for the TSDC measurement. At the end of it, the sample was weighed again and placed in a vacuum oven at T = 95°C for 24 h to determine its dry weight. The mean value of sample weight before and after the measurement was used to determine its water content.

To assess the importance of cytoplasmic glass formation to anhydrous biology, axes of acorn (*Quercus borealis* L.) seeds have been used in this study. Acorn produces "recalcitrant" or unorthodox seeds; these seeds must maintain a relatively high water content to remain viable, and they do not tolerate drying below h = 0.3 (g/g) (21; C. W. Vertucci, personal communication). The comparison between dehydration tolerant soybean with dehydration intolerant acorn can thus provide additional information on the relevance of intracellular glass formation to the proposed mechanism of survival.

Acorn seeds were collected a few days after they were dispersed, and they were kept at 5°C until used. Axes were excised, and their water content was adjusted by rapid drying at room temperature. Rapid drying was achieved by means of a continuous air flow passing through a fine-mesh nylon supporting the excised axes (22). After this drying treatment, samples weighing ~300 mg were immediately used for TSDC and dry weight measurements as described above.

The TSDC method has been extensively described (19, 20, 23). It consists of measuring, during controlled heating, the current generated by the release of a polarized state in a dielectric sandwiched between two electrodes. Samples at a given water content are polarized by an applied electric direct current (DC) field (E_p) at a temperature T_p for a time t_p. This polarization is subsequently frozen in by cooling the sample down to a temperature sufficiently low to prevent depolarization by thermal energy. The field is then switched off. The sample is short circuited through an electrometer and warmed up at a constant rate while the depolarization current is measured. A current peak will thus be observed at a temperature where dipolar disorientation, ionic migration, or carrier release from traps is activated. The use of insulating electrodes prevents injection of charges along with peaks arising from space charge polarization connected with the DC conductivity of the sample. In the case of dipole disorientation with a single relaxation time, obeying the Arrhenius equation

$$\tau(T) = \tau_0 \exp\left(\frac{E_a}{kT}\right) \quad (1)$$

the depolarization current $I(T)$ is expressed as

$$I(T) = \frac{Q}{\tau_0} \exp\left(\frac{-E_a}{kT}\right) \exp\left[\frac{-1}{\beta\tau_0} \int_{T_0}^{T} \exp\left(\frac{-E_a}{kT'}\right) dT'\right] \quad (2)$$

where Q is the area under the peak, τ_0 is the preexponential factor, E_a is the activation energy of dipolar disorientation, k is the Boltzmann's constant, β is the heating rate, and T_0 is the temperature at which the depolarization current starts to appear (24). The activation energy and the preexponential factor can be determined using approximations based on the shape of the TSDC peaks and on evaluation of the integral appearing in the exponential in Eq. 2 (25, 26), as described in the Appendix. These approximations have been used in this study to provide initial guesses for a computer curve-fitting analysis for each peak. The iterative curve-fitting procedure used has been written in collaboration with WaveMetrics (Lake Oswego, OR) and inserted as a macro in a commercially available software (Igor, WaveMetrics). The procedure provides values for activation energy and preexponential factor, along with their standard deviations, for isolated TSDC peaks. Thus, four parameters, namely, temperature of peak maximum (T_m), area under the peak (Q), activation energy (E_a), and preexponential factor (τ_0) can be obtained for each peak in the TSDC spectrum. The contribution of a peak to the static permittivity, $\Delta\epsilon$, can be evaluated from

$$\Delta\epsilon = \frac{Q}{A\epsilon_0 E_p} \quad (3)$$

where A is the cross-sectional area of the sample, and ϵ_0 is the permittivity of free space.

We used a standard cryostat for TSDC measurements. It consists of a sample holder and a dewar containing liquid nitrogen. The sample holder consists of two brass electrodes of 20 mm diameter in a hollow cylindrical brass block. Teflon spacers electrically insulate the electrodes from the cylinder brass block. The cylindrical brass block has three important functions. First, it holds the electrodes and the sample in tight contact with a heating unit. Second, it assures uniform sample heating. Third, it provides a guard-ring configuration so that there is zero potential along one surface of the sample. The two electrodes have different functions. The bottom electrode, which we call the polarizing electrode, is connected to a single-pole, double-throw switch and can be connected either to ground or to a polarizing voltage source, as in a home-built variable DC power supply. The upper electrode, which we call the measuring electrode, is connected to ground through a sensitive electrometer (Keithley 617; Keithley Instruments Inc., Cleveland, OH). The upper electrode can be moved to adjust for sample thickness. Both electrodes are electrically insulated from the sample either by interposing thin foils of mica or Teflon or by using Teflon-coated electrodes. The temperature is measured by a copper-constantan thermocouple placed in proximity of the upper electrode and connected to a digital thermometer (model DP11; Omega Engineering, Stamford, CT). Current and temperature data are recorded and stored by means of a personal computer that simultaneously drives the heating unit through a programmable power supply (LH124; Lambda Electronics Inc., Melville, NY), according to a set heating scheme. During a typical run, 20 data (current and temperature) points were collected every 6 s. Error bars in Fig. 1 indicate standard deviations. Typical values were 3 kV/cm for the polarizing field E_p, 300 K for the polarizing temperature T_p, 5 min for the polarization time t_p . 0.2 K/s for the cooling rate, and 0.05 K/s for the heating rate β. Typical uncertainties were ±1 K in the peak temperature T_m, ±0.02 eV in the activation energy E_a, a factor of ~3 in τ_0, ±10% in $\Delta\epsilon$, and ±0.005 g/g in the sample water content h. Error bars in Figs. 5, 6, and 7 indicate standard deviation of calculated parameters.

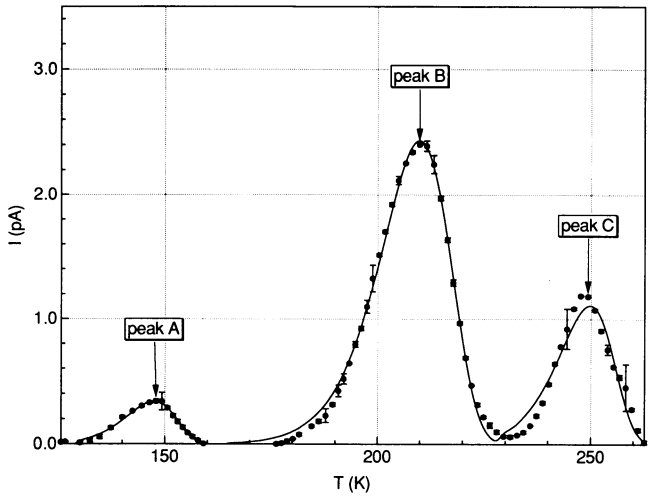

FIGURE 1 Typical TSDC spectrum obtained with a sample of soybean axes with h = 0.15 g/g. Error bars indicate standard deviations. Solid line represents the fit of Eq. 4.2 to data.

RESULTS AND DISCUSSION

An example of a characteristic TSDC spectrum for soybean axes is shown in Fig. 1, along with the results of our curve-fitting procedures. Three main peaks are detected, and we will call them peak A, peak B, and peak C in order of increasing temperatures. The overall quality of the fit is good, given the complexity of the samples and, more importantly, the initial assumption of a single relaxation time for each relaxation process. However, the large values for the peak width at half maximum (~20 K) and deviations in the low temperature tail of each peak suggest a multiplicity of relaxation times representing different relaxation processes. It is thus possible that each peak arises from a convolution of several processes with a distribution of relaxation times and/or activation energies. The values for activation energy reported in this paper should be thus considered only as most probable values, and clearly, further experimental work is required to determine its distribution.

The agreement between the experimental data and Eq. 2 suggests that peaks A, B, and C are due to dipolar disorientation. To confirm this assignment, we must exclude peaks arising from space charge relaxation of free-charge carriers cumulated at the electrode surfaces, all other possible relaxation mechanisms being excluded because of the use of insulating electrodes. Space charge relaxation of charges cumulated at the electrode surfaces give rise to peaks that can be described by an equation similar to Eq. 2 (24). It is clear then that a good fit between Eq. 2 and experimental data is only a necessary condition, but not a sufficient one, for a process to be proved of dipolar origin. To do so, we studied the dependence of the peak temperature, T_m, and amplitude, I_m, on the polarizing field E_p for a soybean sample at h = 0.096 g/g. The same sample has been used for this test,

TABLE 1 **Maximum peak temperatures (T_m) and widths at half amplitude (ΔT) as a function of the polarizing field E_p**

E_p	T_{mA}	ΔT_A	T_{mB}	ΔT_B	T_{mC}	ΔT_C
kV/cm			*K*			
1	144	24	219	22	276	12
2	145	24	218	24	—	—
3	145	26	221	28	—	—
4	143	27	222	38	—	—

and the polarization temperature and time (T_p = 297 K, t_p = 5 min) were kept constant in all the runs. The rationale is that the position of a dipolar peak does not depend on the polarizing field, whereas the peak amplitude is linearly dependent on it. As shown in Table 1, the temperatures of peaks A and B do not depend on the field E_p; interestingly, peak C, present in the first run, disappears from the spectrum in the following runs (Fig. 2). In other words, temperature cycling, and 5 min isothermal temperature treatment at T = 297 K to polarize the sample, eliminated the relaxation process responsible for this current peak. This important fact provided a first indication that peak C might be due to a glass-like transition, the rationale being that the glassy state is a metastable state, and the way in which a lower energy equilibrium state is reached depends solely on the thermal history of the sample (17). On the other hand, during TSDC measurements, polarization of the sample would have induced space charge cumulation on the electrodes in the runs after the first one. The absence of this relaxation mechanism allows us to completely rule out the possibility that peak C might be due to space

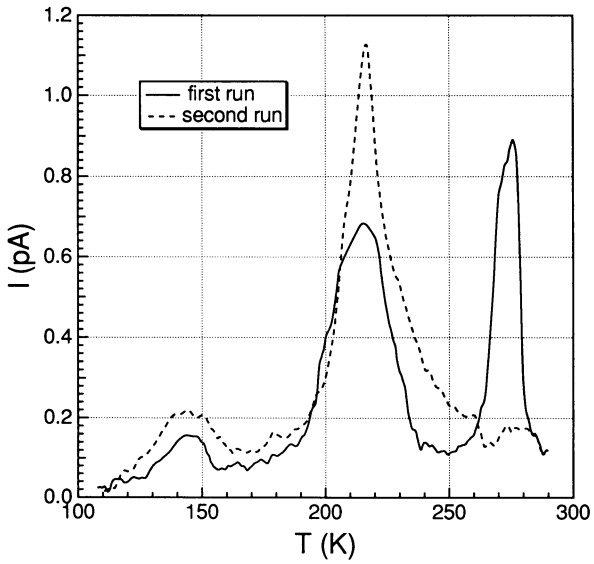

FIGURE 2 TSDC spectra for a soybean axes sample at h = 0.096 g/g. Polarization temperature T_p = 297 K. Polarizing field E_p was 1 kV/cm in the first run and 2 kV/cm in the second run. Peak C disappears on temperature cycling and isothermal treatment at $T = T_p$.

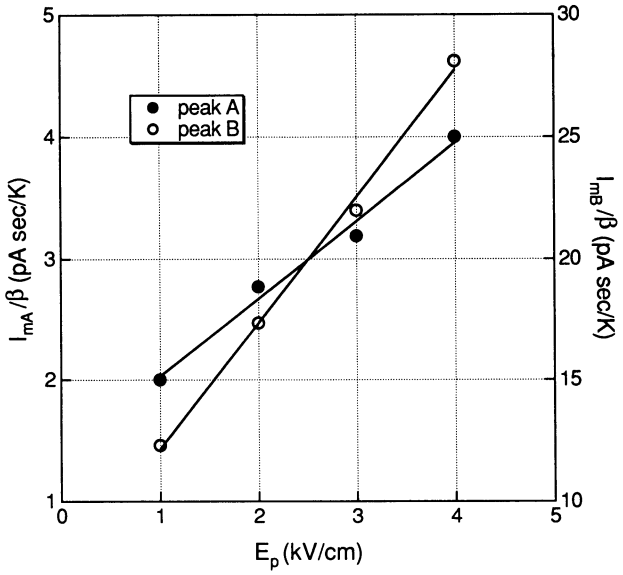

FIGURE 3 Peak amplitude (I_m), normalized by heating rate β, plotted vs. polarizing voltage (E_p) for peak A (●) and peak B (○).

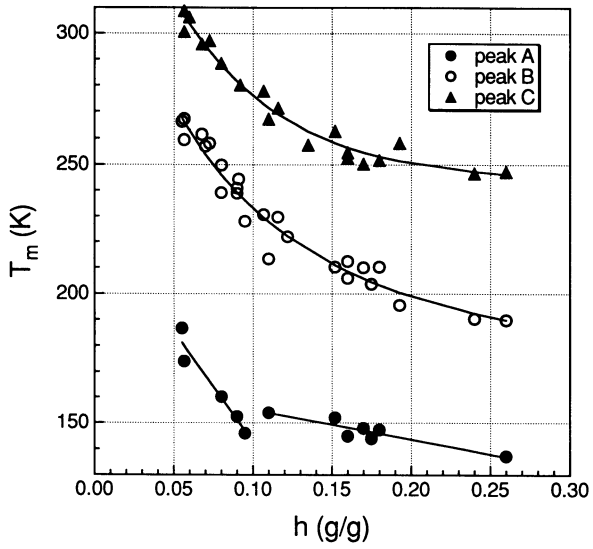

FIGURE 4 Water content dependence of the temperature of the peak maximum (T_m) for peak A (●), peak B (○), and peak C (▲) for soybean axes. Solid lines represent best fit to the data.

charge relaxation phenomena. Further information about the nature of the process represented by peak C will be discussed later.

The width of the peak at half maximum, ΔT, for peaks A, B, and C (ΔT_A, ΔT_B, and ΔT_C, respectively) is included in Table 1. The increase of ΔT_A and ΔT_B during the test suggests an increase of the distribution of relaxation times for the relaxation process and/or an increase in the number of relaxing units. As shown in Fig. 3, the amplitudes for peaks A and B (normalized by the heating rate β) are linearly dependent on the polarizing field. These results strongly support the dipolar nature of peaks A and B and allow us to eliminate the possibility of space charge phenomena.

We have investigated the water content dependence of the temperature of the peak maximum (T_m) for peaks A, B, and C by using soybean axes samples in the hydration range $0.05 < h < 0.30$ g/g. The results are shown in Fig. 4. All three peaks are affected by sample hydration in a similar manner, namely, their T_m decreases with increasing water contents. This indicates that the three different relaxation mechanisms get faster with increasing hydration. In what follows, we will analyze each peak individually, both in terms of its activation energy, E_a, and of its contribution to the static permittivity, $\Delta\epsilon$.

Peak A

The low temperature and small size of the dielectric dispersion indicated by peak A suggest that the process is governed by low activation energy and by a small number of relaxing units. The water dependence of T_m for peak A shows a discontinuity at about $h = 0.12$ g/g (Fig. 4); this anomaly is consistent with the appearance of a new relaxation mechanism at this water content.

The same anomaly is indicated by the $\Delta\epsilon$ and E_a values plotted in Fig. 5 as a function of water content h. Although the static permittivity is slightly decreasing with rising water content for $h \leq 0.12$ g/g, it increases with water content above this value. The activation energy increases with h, reaches a maximum (~0.5 eV) for $h = 0.12$ g/g, and then starts decreasing with increasing hydration, until it levels off at ~0.15 eV. These activation energy values are in the range of reported values for the rotation of a water molecule around a single hydrogen bond (27). TSDC studies with ice samples indicated the presence of a dipolar relaxation mechanism at $T = 125$ K, with activation energies of ~0.25 eV (28–30). Moreover, Seewaldt et al. (31), using nuclear magnetic resonance spectroscopy, reported the appearance of

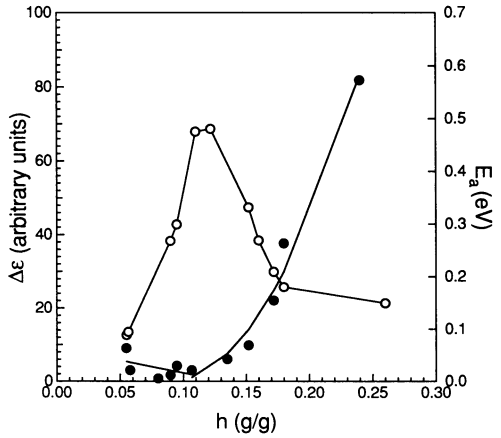

FIGURE 5 Static permittivity $\Delta\epsilon$ (●) and activation energy E_a (○) plotted as a function of water content h for peak A.

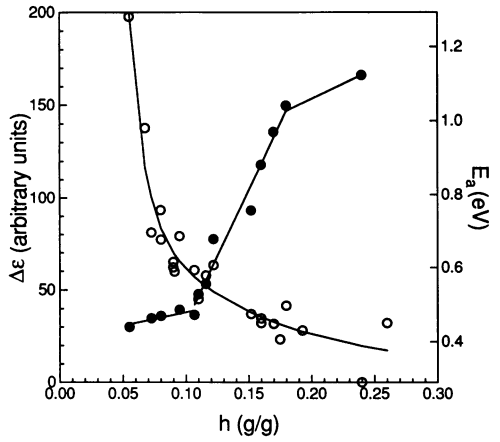

FIGURE 6 Static permittivity $\Delta\epsilon$ (●) and activation energy E_a (○) plotted as a function of water content h for peak B.

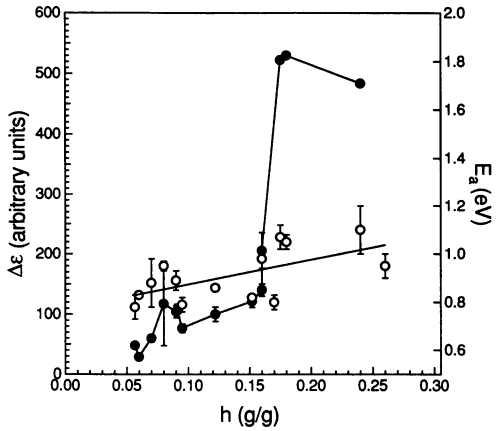

FIGURE 7 Static permittivity $\Delta\epsilon$ (●) and activation energy E_a (○) plotted as a function of water content h for peak C.

water molecules in soybean seed tissue capable of undergoing fast reorientation at just the same hydration level (h = 0.12 g/g) at which $\Delta\epsilon$ starts to increase. Additionally, this water content defines the boundary between a region of very tight and intermediate water binding in soybean axes (32). Using the TSDC method, Pissis (33) showed the existence of a dielectric dispersion in plant leaves and stems, similar to the one indicated by peak A, and he attributed it to the relaxation of loosely bound water molecules.

The above evidence supports the following interpretation: the dipolar relaxation responsible for peak A is attributable to reorientation of unfreezable water molecules bound to other water molecules and/or polar groups on intracellular surfaces through hydrogen bonding. The appearance of this domain of water molecules coincides with the appearance of the relaxation process, and, above h = 0.12 g/g, the magnitude of this relaxation process grows with further hydration.

Peak B

Data for peak B (Figs. 4 and 6) show the dipolar relaxation getting faster and activation energy gradually decreasing with increasing hydration from a value of 1.3 eV at the lowest water content to 0.3 eV at the highest one. The amplitude of the peak increases continually with increasing water content. The increase is significant above h = 0.11 g/g, and it appears to level at higher hydration. Peak temperature values (Fig. 4), and their water dependence, are in excellent agreement with same values reported by Pissis and co-workers (34–36) in TSDC studies of aqueous solutions and solid samples of cellulose and saccharides. This dielectric dispersion has been attributed to rotation of CH_2OH groups, plasticized by water molecules. It is important to realize that soluble sugars constitute a large component of anhydrous biosystems, and in plant seeds they can be present up to 20% of the sample dry weight (37, 38). We can thus suggest that the dipolar relaxation responsible for peak B is mainly governed by hydrated CH_2OH groups.

Peak C

Data for peak C are shown in Figs. 4 and 7. The static permittivity $\Delta\epsilon$ displays a very significant increase at h = 0.17 g/g, and it appears to level off at higher water contents. Conversely, the activation energy is not strongly dependent on sample hydration. It is interesting to notice that although peak B is the largest among all the other peaks in the hydration region $0.05 < h < 0.15$, peak C becomes the largest at higher water contents. Moreover, the dramatic amplitude increase of this latter peak occurs at the same water content at which a 10% increase of the membrane bilayer spacing has been observed in the same anhydrous biosystem (31).

Using an electron spin resonance (ESR) spin probe, the existence of an aqueous glass domain in the cytoplasm of soybean axes has been detected recently (15), and a phase-diagram relating glass transition temperature (T_g) to sample water content was obtained. Fig. 8

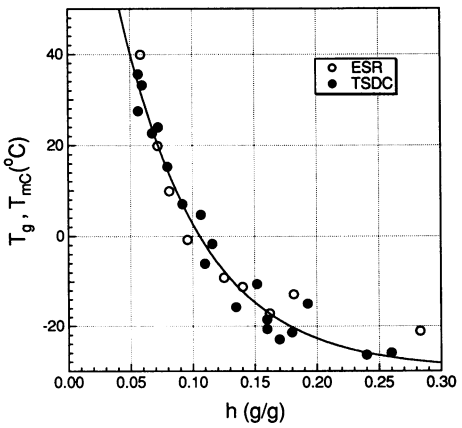

FIGURE 8 Peak C temperature T_m (●) and glass transition temperature T_g (○) obtained with ESR plotted as a function of water content h for soybean axes. Data for T_g are taken from reference 15.

shows peak C temperatures (T_{mC}), along with the above ESR data, as a function of water content h. The good agreement between the two data sets provides further support to the assessment of the relaxation mechanism, responsible for peak C, as a glass transition. Moreover, using differential scanning calorimetry, glass formation in maize embryo (14) and pea axes (39) has been reported, and these data are consistent with both ESR and TSDC data. Additional insight about the nature of this aqueous glass domain has been recently provided by Koster (16). In this study, the glass transition temperature of sugar mixtures, representative of the sugar composition of desiccation tolerant plant seeds, was investigated as a function of hydration. The obtained phase diagram is in fair agreement with ESR, TSDC, and differential scanning calorimetry data collected on intact samples.

It should be noted that calorimetric studies on glass-forming solutions (40–42) showed the presence of freezable (bulk) water after isothermal annealing. As previously mentioned, freezable or bulk water should give rise to a TSDC peak at ~125 K as found in studies on ice samples (28–30), but no freezable water has been found in soybean samples after isothermal annealing (Fig. 2). Thus, we need to assume that water molecules, whose dipolar reorientation is responsible for peak C, will be trapped in a glassy matrix until this is liquefied above T_g, but they will remain unfreezable and behave as dipoles in peaks A and B when the sample is cooled again. This could explain the disappearance of peak C on isothermal annealing above T_g. The width increase of peaks A and B with the number of TSDC runs on the same sample (Table 1) supports the above interpretation.

The possibility to "anneal" the relaxation mechanism responsible for peak C, as indicated in Fig. 2, along with the above data not only strongly support the claim that peak C is associated with a glass transition but also provide strength to the proposed existence of a sugar-water domain that undergoes a glass transition even at room temperatures.

Model for Cell Water

The aim of this study was to investigate the properties of domains of water molecules in biological systems. Within the hydration range considered in this work, three pools of H_2O molecules can be distinguished in soybean samples on the basis of their activation energies for dielectric relaxation (Figs. 4–7). Using the information gained with TSDC, as well as data from the literature, we will propose a model describing interactions of water molecules with cellular constituents.

The model is based on a "patch-like" configuration of water molecules around macromolecules, or macrostructures. The model calls for the existence of several domains of H_2O molecules around the primary hydration sites, approaching the behavior of bulk (free) water with increasing distance from the hydration sites. With TSDC, within the considered hydration range, one can see the hydration shell composed by two domains. The properties of the first domain are described by peak A, whose behavior is consistent with dipolar reorientation of H_2O molecules hydrogen-bonded to other water molecules and/or polar groups on intracellular proteins and membranes. Peaks B and C reflect the properties of an aqueous sugary domain possibly in close proximity with the substrate. The relaxation mechanisms evidenced by TSDC peaks B and C can be thus respectively assigned tentatively to dipolar relaxation of CH_2OH groups of saccharides and to a glass transition in a glassy domain around solid intracellular surfaces.

It is clear that we are implicitly assuming that sugar-water domains surround solid intracellular surfaces. This latter assumption finds strong supporting evidence in studies on lipid-sugar (43, 44), as well as protein-sugar interactions (45), and it has been shown that carbohydrates can stabilize membrane bilayers and proteins during extreme dehydration, by direct interaction of sugar hydroxyls with polar headgroup of dry phospholipids and polar groups of proteins. These conclusions led Crowe and associates (45a) to formulate the "water replacement hypothesis" (WRH), based on the possibility that polyhydroxyl compounds can replace the structural water of cellular components as intracellular water levels are reduced, thereby preventing a variety of potential lethal events from taking place (6). According to the WRH hypothesis, using TSDC we should have been able to detect this release of water molecules from intracellular surfaces, as manifested by an increase of the amplitude of peak A below a given water content. The small increase in peak A amplitude, as well as the decrease of activation energies below h = 0.12 g/g (Fig. 5), may support the WRH model.

Nevertheless, differences have been observed among sugars (for example, trehalose, maltose, sucrose, and glucose in order of efficacy) in protecting membrane bilayers and proteins against dehydration (45). Still, there is no clear structural explanation for the relative efficiency of different sugars, except that it is not related to the number or position of hydroxyl groups available for hydrogen bonding (46). Green and Angell (47) recently have investigated the possibility that the above-mentioned order of efficacy could be connected with the glass-forming characteristics of the aqueous saccharide solutions. Their results indicate indeed that the order of efficacy is linked to the glass-forming ability of sugars, namely, the higher the glass transition temperature of a saccharide at a given water content, the more efficient it is as a dehydration protectant (47).

Therefore, the important point should be made here that the ability of saccharides to protect intracellular structures against dehydration is strictly connected with their ability to form or to induce glass formation at physiological temperatures (47).

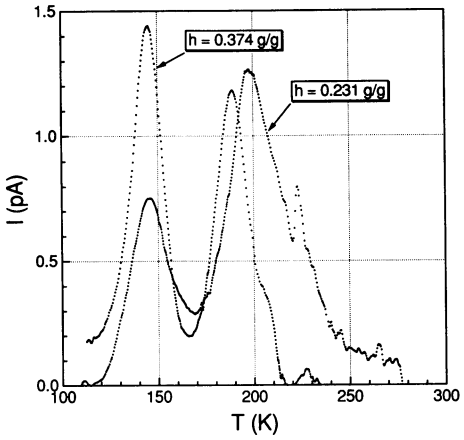

FIGURE 9 TSDC spectra for two samples of acorn axes at the water content indicated. Polarization temperature T_p = 298 K, and polarizing field E_p = 4 kV/cm.

Dehydration intolerant seeds

Fig. 9 shows TSDC spectra obtained with two samples of acorn seed axes at the water contents indicated. As mentioned in the Materials and Methods section, acorn seed axes are tolerant to dehydration only up to about $h = 0.3$ g/g (21; C. W. Vertucci, personal communication). Thus, the sample at $h = 0.374$ g/g is still germinable, whereas the sample at $h = 0.231$ g/g is ungerminable. Two peaks are evident in both spectra: a low temperature peak at about $T = 145$ K, whose position does not change with water content, and a peak at about $T = 200$ K, whose maximum temperature shifts to lower values with increasing hydration. A comparison of the peak maximum temperature and water content for these two peaks with the same parameters for peaks A, B, and C (Fig. 4), obtained for soybean axes, clearly indicates the two peaks observed for acorn axes as being consistent with peaks A and B. A current peak with position and size similar to peak C is completely missing in the dehydration intolerant organism. This important point strongly indicates the existence of cytoplasmic glassy domains as a key factor for the ability of anhydrobiotic organisms to tolerate desiccation.

Nevertheless, we have to account for the presence of saccharides in acorn axes, as indicated by the relatively large current peak with characteristics similar to peak B observed in soybean axes and attributed to dipolar relaxation of hydrated CH_2OH groups. It is interesting to notice that the transition temperature for glass-forming monosaccharides is ~30 K lower compared with glass-forming oligosaccharides at the same water content (16, 47, 48). It is thus reasonable to assume that the small current peak visible at about $T = 225$ K for the acorn sample at $h = 0.231$ g/g, and the shoulder at about $T = 210$ K for the acorn sample at $h = 0.374$ g/g (Fig. 9), indicates the presence of a monosaccharide glassy domain, as suggested by peak C being at $T = 240$ K in the same hydration range (Fig. 4). The relatively low efficacy of monosaccharides in protecting membranes and proteins against dehydration, as discussed above, would thus account for acorn seeds being unable to tolerate dehydration.

The low temperature peak observed for acorn axes is relatively large compared with peak A (Figs. 1 and 9). This suggests that in dehydration intolerant biosystems a large fraction of cell-associated water is hydrogen bonded to other water molecules and/or polar groups on intracellular surfaces and does not participate in glassy domains.

CONCLUSIONS

The data presented in this study provide evidence of populations of water molecules at biological interfaces and suggest that these domains exist discretely within a cell. The distinctive physical properties of these pools are consequences of their specific interactions with cell constituents. The crucial importance of glassy domain around intracellular surfaces must be underlined once more; although it preserves the structures, it prevents their functioning by replacing relatively mobile water molecules with immobile solutes. This is an equally important role in stabilizing the dried cell.

A recent study on the changes in the thermal properties of water pools in soybean seeds (7) indicated the existence of five hydration levels in the hydration range $0 < h < 1$ g/g. The hydration range considered in the present study for soybean axes overlaps with one of the reported hydration levels, namely, hydration level 2 ($0.08 < h < 0.21$ g/g). Our results thus imply that relevant differences on the state of water molecules exist within one of the reported hydration levels. Clearly, this provides further proof for the ability of TSDC to resolve complex relaxation mechanisms.

The proposed model for cell-associated water is suggestive of a previous model based on the occurrence of interfacial water ("vicinal water"), usually near a solid surface, the properties of which differ from the corresponding bulk properties due to structural differences induced by the proximity of the surface (49). The two models can still concord if the effect of surfaces on vicinal water could be considered as resulting from the presence of glassy domains. Clearly, further studies are needed to confirm this assumption.

Questions arise about the unusual features of anhydrous biosystems, allowing for the possibility that conclusions and models derived from their study may have limited or even no general applicability. Obviously, these organisms do have abilities that most organisms do not, notably their ability to reversibly dehydrate. Nevertheless, the understanding of the physical and chemical mechanisms by which anhydrobiotic organisms tolerate extreme dehydration may shed light and provide hints to improve technologies in seed storage, gene banks, and in

the preservation of dry foods and pharmaceutical products.

APPENDIX

Evaluation of TSDC peak parameters

This appendix will illustrate the method used to evaluate activation energies (E_a) and preexponential factors (τ_0) for thermally stimulated depolarization current experiments. The method is based on an approximation suggested by Christodoulides et al. (50).

The equation describing first-order thermally stimulated processes, known as the Randall-Wilkins equation, has been shown to describe current peaks due to dipolar disorientation as observed in TSDC experiments (51, 52). The depolarization current as a function of temperature $I(T)$ is, for a constant heating rate β,

$$I(T) = \frac{Q}{\tau_0}\exp\left(\frac{-E_a}{kT}\right)\exp\left[\frac{-1}{\beta\tau_0}\int_{T_0}^{T}\exp\left(\frac{-E_a}{kT'}\right)dT'\right] \quad \text{(A1)}$$

where Q is the area under the current peak, τ_0 is the preexponential factor, E_a is the activation energy of the dipolar disorientation process, k is the Boltzmann's constant, and T_0 is the temperature at which the depolarization current peak starts to appear. The maximum depolarization current occurs at a temperature T_m, according to

$$T_m = \left[\frac{\beta E_a}{k}\tau_0\exp\left(\frac{E_a}{kT_m}\right)\right]^{1/2} \quad \text{(A2)}$$

Eq. A1 can be rewritten as

$$I(T) = \frac{Q}{\tau_0} \times \exp\left[-\frac{E_a}{kT} - \left(\frac{E_a}{kT_m}\right)^2\exp\left(\frac{E_a}{kT_m}\right)\int_{E_a/kT}^{\infty}\frac{e^{-z}}{z^2}dz\right] \quad \text{(A3)}$$

The integral appearing in Eq. A3 can be expressed in terms of the function $H(x)$ (53) as

$$H(x) = \int_1^{\infty}\frac{e^{-xt}}{t^2}dt = x\int_x^{\infty}\frac{e^{-z}}{z^2}dz \quad \text{(A4)}$$

$$H(x) \approx \frac{e^{-x}}{x+2}\left[1 + \frac{2}{(x+2)^2} - \frac{4(x-1)}{(x+2)^4} + \cdots\right] \quad \text{(A5)}$$

Eq. A3 can hence be rearranged with the help of Eqs. A4 and A5 as

$$I(T) = \frac{Q}{\tau_0} \times \exp\left[-\frac{E_a}{kT} - \left(\frac{E_a}{kT_m}\right)^2\exp\left(\frac{E_a}{kT_m}\right)\frac{kT}{E_a}H\left(\frac{E_a}{kT}\right)\right]. \quad \text{(A6)}$$

TSDC experiments usually give $x = E_a/kT$ in the range 10–100, with the vast majority of values being in the range 20–50 (50). The results discussed in the preceding paper provide values for E_a/kT well within the above range. In the low temperature region, typical values for E_a and T are 0.25 eV and 150 K, respectively, giving $x \approx 19$. In the high temperature region, typical values for E_a and T are 1 eV and 270 K, respectively, giving $x \approx 43$. In the situations where $x > 5$, one can safely drop all the terms in Eq. A5 except the first one, so that $H(x)$ becomes

TABLE A.1 Values for $H(x)$, $P(x)$, along with their ratio, for x in the range 5–60

x	$H(x)$	$P(x)$	$H(x)/P(x)$
5	$9.63\ 10^{-4}$	$1.35\ 10^{-3}$	0.71
10	$3.78\ 10^{-6}$	$4.54\ 10^{-6}$	0.83
20	$9.37\ 10^{-11}$	$1.03\ 10^{-10}$	0.91
30	$2.92\ 10^{-15}$	$3.12\ 10^{-15}$	0.94
40	$1.01\ 10^{-19}$	$1.06\ 10^{-19}$	0.95
50	$3.71\ 10^{-24}$	$3.86\ 10^{-24}$	0.96
60	$1.41\ 10^{-28}$	$1.46\ 10^{-28}$	0.97

$$H(x) \approx \frac{e^{-x}}{x+2}. \quad \text{(A7)}$$

For values of x in the range 20–50, the error introduced by considering

$$P(x) = \frac{e^{-x}}{x} \quad \text{(A8)}$$

instead of $H(x)$ is negligible, as shown by the ratio $H(x)/P(x)$ in Table A1. By replacing $H(x)$ with $P(x)$, Eq. A6 can be written as

$$I(T) = \frac{Q}{\tau_0}\exp\left[-\frac{E_a}{kT} - \left(\frac{E_a}{kT_m}\right)^2 \times \exp\left(\frac{E_a}{kT_m}\right)\left(\frac{kT}{E_a}\right)^2\exp\left(\frac{-E_a}{kT}\right)\right] = \frac{Q}{\tau_0}\exp\left\{-\frac{E_a}{kT} - \left(\frac{T}{T_m}\right)^2\exp\left[\frac{E_a}{k}\left(\frac{T-T_m}{T_mT}\right)\right]\right\}. \quad \text{(A9)}$$

Eq. A9 is used to fit individual current peak data by means of an iterative curve-fitting software written in collaboration with WaveMetrics. The area under the current peak (Q) is obtained by rectangular integration of raw TSDC data, and initial guesses for the activation energy (E_a) and the pre-exponential factor (τ_0) are provided by the peak area to height ratio, as described by Christodoulides et al. (50). Briefly, the parameter γ

$$\gamma = \frac{I_m T_m}{\beta Q}e \quad \text{(A10)}$$

where I_m is the peak maximum current and e is the base of natural logarithms, is used to calculate approximate values for the activation energy (E') and the pre-exponential factor (τ') according to

$$E' = {}^1/_2(\gamma - 4 + \sqrt{\gamma^2 + 16})kT_m \quad \text{(A11)}$$

$$\tau' = \frac{kT_m^2}{\beta E'}\exp\left(\frac{-E'}{KT_m}\right). \quad \text{(A12)}$$

Received for publication 20 September 1991 and in final form 29 April 1992.

REFERENCES

1. Nimtz, G. 1986. Magic numbers of water molecules bound between lipid bilayers. *Physica Scripta.* T13:172–177.
2. Leopold, A. C., editor. 1986. Membranes, Metabolism, and Dry Organisms. Cornell University Press, Ithaca, NY. 374 pp.
3. Franks, F., and S. F. Mathias, editors. 1982. Biophysics of Water. John Wiley & Sons, New York. 400 pp.
4. Vertucci, C. W., and A. C. Leopold. 1984. Bound water in soybean seeds and its relation to respiration and imbibitional damage. *Plant Physiol.* 75:114–117.
5. Vertucci, C. W. 1989. The effects of low water contents on physiological activities of seeds. *Physiol. Plant.* 77:172–176.
6. Clegg, J. S. 1986. The physical properties and metabolic status of Artemia cysts at low water contents: the "water replacement hypothesis". *In* Membranes, Metabolism, and Dry Organisms. A. C. Leopold, editor. Cornell University Press, Ithaca, NY. 169–185.
7. Vertucci, C. W. 1990. Calorimetric studies of the state of water in seed tissues. *Biophys. J.* 58:1463–1471.
8. Rupley, J. A., and G. Careri. 1991. Protein hydration and function. *Adv. Protein Chem.* 41:37–172.
9. Bruni, F., G. Careri, and A. C. Leopold. 1989. Critical exponents of protonic percolation in maize seeds. *Physiol. Rev. A* 40:2803–2805.
10. Bruni, F., G. Careri, and J. S. Clegg. 1989. Dielectric properties of Artemia cysts at low water contents. Evidence for a percolative transition. *Biophys. J.* 55:331–338.
11. Bruni, F., and A. C. Leopold. 1991. Hydration, protons and onset of physiological activities in maize seeds. *Physiol. Plant.* 81:359–366.
12. Burke, M. J. 1986. The glassy state and survival of anhydrous biological systems. *In* Membranes, Metabolism, and Dry Organisms. A. C. Leopold, editor. Cornell University Press, Ithaca, NY. 358–364.
13. Vertucci, C. W. 1989. Effects of cooling rate on seeds exposed to liquid nitrogen temperatures. *Plant Physiol.* 90:1478–1485.
14. Williams, R. J., and A. C. Leopold. 1989. The glassy state in corn embryos. *Plant Physiol.* 89:977–981.
15. Bruni, F., and A. C. Leopold. 1991. Glass transitions in soybean seed. Relevance to anhydrous biology. *Plant Physiol.* 96:660–663.
16. Koster, K. L. 1991. Glass formation and desiccation tolerance in seeds. *Plant Physiol.* 96:302–304.
17. Franks, F. 1985. Biophysics and Biochemistry at Low Temperatures. Cambridge University Press, Cambridge. 210 pp.
18. Vertucci, C. W., and A. C. Leopold. 1986. Physiological activities associated with hydration level in seeds. *In* Membranes, Metabolism, and Dry Organisms. A. C. Leopold, editor. Cornell University Press, Ithaca, NY. 35–49.
19. van Turnhout, J. 1987. Thermally stimulated discharge of electrets. *In* Electrets. G. N. Sessler, editor. Springer-Verlag, Berlin. 81–215.
20. Mascarenhas, S. 1987. Bioelectrets: electrets in biomaterials and biopolymers. *In* Electrets. G. M. Sessler, editor. Springer-Verlag, Berlin. 321–346.
21. Bewley, J. D., and M. Black. 1985. Seeds. Physiology of Development and Germination. Plenum Press, New York. 367 pp.
22. Pammenter, N. W., C. W. Vertucci, and P. Berjak. 1991. Homeohydrous (recalcitrant) seeds: dehydration, the state of water and viability characteristics in *Landolphia kirkii. Plant Physiol.* 96:1093–1098.
23. Bucci, C., and R. Fieschi. 1966. Ionic thermocurrents in dielectrics. *Physiol. Rev.* 148:816–823.
24. Vanderschueren, J., and J. Gasiot. 1979. Field-induced thermally stimulated currents. *In* Thermally Stimulated Relaxation in Solids. P. Braünlich, editor. Springer-Verlag, New York. 135–223.
25. Prakash, J., Rahul, and A. K. Nishad. 1986. Evaluation of dielectric relaxation parameters from the ionic thermocurrent spectrum. *J. Appl. Physiol.* 59:2129–2135.
26. Christodoulides, C., L. Apekis, and P. Pissis. 1988. Peak parameters from peak area to height ratio in thermally stimulated depolarization and thermoluminescence. *J. Appl. Physiol.* 64:1367–1370.
27. Finney, J. L. 1982. Solvent effects in biomolecular processes. *In* Biophysics of Water. F. Franks and S. F. Mathias, editors. John Wiley & Sons, New York. 55–58.
28. Apekis, L., and P. Pissis. 1987. Study of the multiplicity of dielectric relaxation times in ice at low temperatures. *J. Phys. C1* 48:127–133.
29. Onsager, L., D. L. Staebler, and S. Mascarenhas. 1978. Electrical effects during condensation and phase transitions of ice. *J. Chem. Phys.* 68:3823–3828.
30. Johari, G. P., and S. J. Jones. 1975. Study of the low-temperature "transition" in ice Ih by thermally stimulated depolarization measurements. *J. Chem. Phys.* 62:4213–4223.
31. Seewaldt, V., D. A. Priestley, A. C. Leopold, G. W. Feigenson, and F. Goodsaid-Zalduondo. 1981. Membrane organization in soybean seeds during hydration. *Planta.* 152:19–23.
32. Vertucci, C. W., and A. C. Leopold. 1987. The relationship between water binding and desiccation tolerance in tissues. *Plant Physiol.* 85:232–238.
33. Pissis, P. 1990. The dielectric relaxation of water in plant tissue. *J. Exp. Bot.* 41:677–684.
34. Pissis, P. 1985. A study of sorbed water on cellulose by the thermally stimulated depolarization technique. *J. Phys. D Appl. Phys.* 18:1897–1908.
35. Pissis, P., and D. Daoukaki-Diamanti. 1988. Dielectric study of aqueous solutions and solid samples of methylcellulose. *Prog. Colloid Polym. Sci.* 78:27–29.
36. Pissis, P., and D. Daoukaki-Diamanti. 1986. Dielectric study of sorbed water in galactose. *Chem. Phys.* 101:95–104.
37. Amuti, K. S., and C. J. Pollard. 1977. Soluble carbohydrates of dry and developing seeds. *Phytochemistry.* 16:529–532.
38. Koster, K. L., and A. C. Leopold. 1988. Sugars and desiccation tolerance in seeds. *Plant Physiol.* 88:829–832.
39. Bruni, F., R. J. Williams, and A. C. Leopold. 1990. Vitrified cytoplasm in dry seeds. *Plant Physiol.* 93:S-132. (Abstr. No. 779).
40. MacKenzie, A. P. 1977. Non-equilibrium freezing behavior of aqueous systems. *Phil. Trans. R. Soc. Lond. B Biol. Sci.* 278:167–189.
41. Angell, C. A., and J. C. Tucker. 1979. Heat capacity changes in glass-forming aqueous solutions and the glass transition in vitreous water. *J. Phys. Chem.* 84:268–272.
42. Takahashi, T., and A. Hirsh. 1985. Calorimetric studies of the state of water in deeply frozen human monocytes. *Biophys. J.* 47:373–380.
43. Crowe, J. H., L. M. Crowe, J. F. Carpenter, A. S. Rudolph, C. Aurell-Wistrom, B. J. Spargo, and T. J. Anchordoguy. 1988. Interactions of sugars with membranes. *Biochim. Biophys. Acta.* 947:367–384.
44. Caffrey, M., V. Fonseca, and A. C. Leopold. 1988. Lipid-sugar interactions. Relevance to anhydrous biology. *Plant Physiol.* 86:754–758.

45. Crowe, J. H., L. M. Crowe, J. F. Carpenter, and C. Aurell Wistrom. 1987. Stabilization of dry phospholipids bilayers and proteins by sugars. *Biochem. J.* 242:1–10.

45a. Crowe, J. H. 1971. Anhydrobiosis, an unsolved problem. *Am. Nat.* 105:563–573.

46. Crowe, L. M., R. Mouradian, J. H. Crowe, S. A. Jackson, and C. Womersley. 1984. Effects of carbohydrates on membrane stability at low water activities. *Biochim. Biophys. Acta.* 769:141–150.

47. Green, J. L., and C. A. Angell. 1989. Phase relations and vitrification in saccharide-water solutions and the trehalose anomaly. *J. Phys. Chem.* 93:2880–2882.

48. Williams, R. J. 1991. Changes in glass transition temperatures during germination of pea embryos. *Plant Physiol.* 96:S-62. (Abstr. No. 408).

49. Drost-Hansen, W. 1982. The occurrence and extent of vicinal water. *In* Biophysics of Water. F. Franks and S. F. Mathias, editors. John Wiley & Sons, New York. 163–169.

50. Christodoulides, C., L. Apekis, and P. Pissis. 1988. Peak parameters from peak area to height ratio in thermally stimulated depolarization and thermoluminescence. *J. Appl. Physiol.* 64:1367–1370.

51. van Turnhout, J. 1987. Thermally stimulated discharge of electrets. *In* Electrets. G. N. Sessler, editor. Springer-Verlag, Berlin. 81–215.

52. Chen, R., and Y. Kirsh. 1981. Analysis of Thermally Stimulated Processes. Pergamon Press, Oxford, UK. 361 pp.

53. Abramowitz, M., and I. A. Stegun, editors. 1975. Handbook of Mathematical Functions. Academic Press, New York. 568 pp.